

ARR July 1942

~~SECRET~~
17
NATIONAL ADVISORY COMMITTEE FOR AERONAUTICS
~~CONFIDENTIAL~~

WARTIME REPORT

ORIGINALLY ISSUED
July 1942 as
Advance Restricted Report

WIND-TUNNEL INVESTIGATION OF A PLAIN AILERON

AND A BALANCED AILERON ON A TAPERED WING

WITH FULL-SPAN DUPLEX FLAPS

By F. M. Rogallo and John G. Lowry

Langley Memorial Aeronautical Laboratory
Langley Field, Va.

NACA

WASHINGTON

NACA WARTIME REPORTS are reprints of papers originally issued to provide rapid distribution of advance research results to an authorized group requiring them for the war effort. They were previously held under a security status but are now unclassified. Some of these reports were not technically edited. All have been reproduced without change in order to expedite general distribution.

NATIONAL ADVISORY COMMITTEE FOR AERONAUTICS

ADVANCE RESTRICTED REPORT

WIND-TUNNEL INVESTIGATION OF A PLAIN AILERON
AND A BALANCED AILERON ON A TAPERED WING
WITH FULL-SPAN DUPLEX FLAPS

By F. M. Rogallo and John G. Lowry

SUMMARY

An investigation was made of a plain aileron and a balanced aileron on a tapered wing with full-span duplex flaps, which consisted of an inboard NACA slotted flap and an outboard balanced split flap. The investigation was made in the 7- by 10-foot wind tunnel of the Langley Memorial Aeronautical Laboratory. Increments of maximum lift coefficient of 0.82 and 1.04 were obtained from the inboard flap alone and from the duplex-flap combination, respectively. The aileron was as effective with flaps fully extended as with flaps retracted, but a 30-percent reduction of aileron effectiveness appears unavoidable at intermediate positions of the outboard flap. If this reduction is acceptable, the wing arrangement tested should be satisfactory. Estimated rates of roll and stick forces for the arrangement on a fighter airplane are given.

INTRODUCTION

Increased speed and wing loading of modern airplanes have led to difficulties in obtaining high lifts for landing and take-off without impairing lateral control. In order to obtain solutions for this problem, the NACA is investigating, on a semispan model of the tapered wing of a modern fighter airplane, lateral-control devices that appeared promising from wind-tunnel tests on a rectangular wing with a square tip.

The present tests were made of a plain and a balanced aileron on a wing with full-span "duplex" flaps consisting of an inboard NACA slotted flap and an outboard balanced split flap. This work may be considered an extension of the work reported in reference 1. A similar arrangement is to be flight-tested. The object of the wind-tunnel tests was to determine the lift characteristics and the aileron-control characteristics for various locations of the outboard

L-481

flap and for various amounts of aileron balance.

The stick forces and the rates of roll were estimated for an airplane with the outboard flap in several positions along a particular flap path.

APPARATUS AND METHODS

A semispan wing model was suspended in the 7- by 10-foot wind tunnel (reference 2) of the Langley Memorial Aeronautical Laboratory as shown schematically in figure 1. The root chord of the model was adjacent to one of the vertical walls of the tunnel, the vertical wall thereby serving as a reflection plane. The flow over a semispan in this set-up is essentially the same as it would be over a complete wing in a 7- by 20-foot wind tunnel. Although a very small clearance was maintained between the root chord of the model and the tunnel wall, no part of the model was fastened to or in contact with the tunnel wall. The model was suspended entirely from the balance frame, as shown in figure 1, so that all the forces and moments acting on the model might be determined. Provisions were made for changing the angle of attack while the tunnel was in operation.

The ailerons were deflected by means of a calibrated torque rod connecting the outboard end of the aileron with a crank outside the tunnel wall, the hinge moments being determined from the twist of the rod (fig. 1).

The tapered wing model used in these tests was built to the plan form shown in figure 2(a) and represents the cross-hatched portion of the airplane in figure 2(b). The airfoil sections were of the NACA 230 series tapering in thickness from approximately $15\frac{1}{2}$ percent at the root to $8\frac{1}{4}$ percent at the tip (table I). The basic chord, c_1 , of the wing model was arbitrarily increased 3/10 inch to reduce the trailing-edge thickness and the last few stations were refaired to give a smooth contour.

The slotted flap was built to the ordinates of table II and had a chord of about 20.7 percent of the wing chord. The ordinates are given for the root and tip sections. The flap was cut at the 52.3-inch station for these tests. The slot shape and flap-pivot point are given in table II. The outboard flap, consisting of a constant chord Clark Y airfoil, could be tested with the nose in the positions shown by the grid in figure 2(c). The aileron had provisions for changing the balance and consisted of a 15.5-percent-chord plain aileron with a balance

plate attached to the nose of the aileron (fig. 2(c)). The balance plates were tapered along the span of the aileron to give the maximum balance with the required deflections. The balance chord is the distance from the hinge axis to a point midway between the edges of the seal with aileron neutral.

All tests were made at a dynamic pressure of 9.21 pounds per square foot, which corresponds to a velocity of about 60 miles per hour and to a test Reynolds number of about 1,540,000 based on the mean aerodynamic chord of 33.66 inches.

RESULTS AND DISCUSSION

Coefficients and Corrections

The symbols used in the presentation of results are:

C_L	lift coefficient (L/qS)
C_D	uncorrected drag coefficient (D/qS)
C_m	pitching-moment coefficient (M/qSc')
C_l'	rolling-moment coefficient (L'/qbS)
C_n'	yawing-moment coefficient (N'/qbS)
C_h	aileron hinge-moment coefficient ($H_a/qb_a \bar{c}_a^2$)
ΔC_h	C_h of up aileron minus C_h of down aileron
c	wing chord at any spanwise location with flaps retracted
c'	mean aerodynamic chord
c_a	aileron chord measured along airfoil-chord line from hinge axis of aileron to trailing edge of airfoil
c_b	balance chord measured from hinge axis to point midway between seal edge with ailerons neutral
\bar{c}_a	root-mean-square chord of the aileron
\bar{c}_b	root-mean-square chord of aileron balance
\bar{c}_b/\bar{c}_a	balance ratio

b	twice span of semispan model
b _a	aileron span
S	twice area of semispan model
L	twice lift on semispan model
D	twice drag on semispan model
M	twice pitching moment of semispan model about support axis
L'	rolling moment, due to aileron deflection, about wind axis in plane of symmetry
N'	yawing moment, due to aileron deflection, about wind axis in plane of symmetry
H _a	aileron moment about hinge axis
q	dynamic pressure of air stream $(1/2 \rho V^2)$ uncorrected for blocking
V	free-stream velocity
α	angle of attack
δ_a	aileron deflection relative to wing, positive when trailing edge is down
δ_{f_1}	inboard flap deflection relative to wing, positive when trailing edge is down
δ_{f_2}	angle between chord line of wing and lower surface of outboard flap
C_{l_p}'	rate of change of rolling-moment coefficient C_l' with helix angle $p b / 2V$
p	rate of roll
F _s	stick force

A positive value of L' or C_l' corresponds to an increase in lift of the model, and a positive value of N' or C_n' corresponds to a decrease in drag of the model. Twice the actual lift, drag, pitching moment, area, and span of the model was used in the reduction of the results because the model represented half of a complete wing. The

drag coefficient and the angle of attack have been corrected only in accordance with the theory of trailing-vortex images. Corresponding corrections were applied to the rolling- and yawing-moment coefficients. No corrections have been applied to the hinge-moment coefficients, and no corrections have been applied to any of the results for the effects of the support strut or the treatment of the inboard end of the wing; that is, the small gap between the wing and the wall, the leakage through the wall around the support tube, and the boundary layer at the wall. It is believed that the drag values are only comparative and are not directly applicable to performance estimations.

Lift Characteristics

Contours of the location of outboard-flap nose for maximum lift coefficient of the wing with inboard and outboard flaps deflected 50° and 40° , respectively, are shown in figure 3. An increase of maximum lift coefficient is apparent as the flap is moved back to the aileron axis. Vertical location of the flap had little effect on the maximum lift coefficient over the range of locations tested but would probably have an important effect in more rearward locations and with gaps of less than 0.04c, as shown on figure 4 of reference 3.

The chordwise location of the deflected outboard-flap nose appears to have a greater effect on the pitching-moment coefficient than upon the lift or drag coefficients. (See fig. 4(a).) The results of tests with aileron neutral and with the outboard-flap nose 2-, 4-, and 6-percent c below the wing contour at positions 4 and 5 showed very little effect of vertical location upon lift, drag, or pitching-moment coefficients. The results with only the large gaps are presented. The angular setting of the extended outboard flap had a considerable effect upon all the characteristics, as shown in figure 4(b).

The maximum lift coefficients obtained with flaps neutral, with partial-span slotted flap deflected 50° , and with duplex flaps deflected 40° were 1.40, 2.22, and 2.44, respectively. The values of $C_{L_{max}}$ for the three flap conditions are expected to increase as the

Reynolds number is increased to full scale. The increments of $C_{L_{max}}$ due to the flaps may also change with scale because of a change in the location and progression of the stall. Neither the effect of scale nor of the tunnel boundaries upon the stall of the wing was investigated.

Aileron Characteristics

Aileron with $0.333\bar{3}_a$ balance.— When the outboard flap was retracted, the aileron with $0.333\bar{3}_a$ balance was limited to deflections

of $\pm 14^\circ$. With these aileron deflections, the maximum rolling-moment coefficient was found to depend critically upon the position and deflection of the outboard flap, as shown in figure 5. A study of the contours of figure 5 indicates that, although there need be no loss in rolling-moment coefficient with the flaps fully extended relative to the flap-retracted condition, a reduction of aileron effectiveness during extension of the outboard flap appears to be inevitable. The reduction need be no more than about a third of the flap-neutral value, however, if the flap path is properly chosen. The rolling-, yawing-, and hinge-moment coefficients of the aileron with both flaps retracted, with the inboard flap fully deflected and the outboard flap retracted, and with the inboard flap fully deflected and the outboard flap at several positions along a promising flap path are given in figure 6. It is believed that the fairing of the hinge-moment coefficient curves of figure 6 is more nearly correct than point-to-point fairing because of the small clearances in the aileron system and unavoidable friction. Rates of roll and stick forces based on these data will be presented later.

Aileron with $0.415\bar{c}_a$ balance.- Tests of the aileron with $0.415\bar{c}_a$ balance were made primarily to determine the effect of balance upon the hinge-moment coefficient. A comparison of these data (fig. 7) with the data of figure 6(a) shows that the reduction of $\partial C_h / \partial \delta_a$ was the principal effect of the increase of balance, as was to be expected. With this balance it was anticipated that a deflection range of $\pm 12^\circ$ would be obtained but, through an error in construction, the range obtained was from 5° to -14° . It was not considered worth while to alter the model, because the desired information may be obtained by comparing the hinge moment of this aileron with that of other ailerons over the same deflection range.

Plain sealed aileron.-The characteristics of the plain sealed aileron on the wing with flaps retracted are given in figure 8(a) and with the outboard flap in several positions but at a single angle of attack, in figure 8(b). These data provide a basis of comparison for the determination of the effectiveness of the internal balances and an extension of the rolling- and yawing-moment coefficients to higher aileron deflections than were possible with the internal balances.

Effect of balance upon $\partial C_h / \partial \alpha$ and $\partial C_h / \partial \delta_a$.- The aileron hinge-moment slopes $\partial C_h / \partial \alpha$ and $\partial C_h / \partial \delta_a$ for the three amounts of balance tested are compared in figure 9. The values of $\partial C_h / \partial \delta_a$ given were estimated for the aileron range of 5° to -5° at angles of attack of 0° and 13° , and the values of $\partial C_h / \partial \alpha$ were estimated for the α ranges of approximately -4° to 4° and 9° to 17° with aileron neutral. It will be noticed that the numerical values of both derivatives are

considerably greater in the high angle-of-attack range than in the high-speed range.

Estimated Rates of Roll and Stick Forces

The rates of roll and the stick forces during steady rolling for the airplane shown in figure 2(b) have been estimated from the data of figure 6. (See fig. 10.) The rates of roll were estimated by means of the relationship

$$pb/2V = C_{l_p}'/C_{l_p} \quad (1)$$

where C_{l_p}' , the coefficient of damping in roll, was taken as 0.46 from the data of reference 4. Wing twist has been neglected. The stick forces were estimated from the relationship

$$F_S = 60 \Delta C_h / C_L \quad (2)$$

which may be derived from the aileron dimensions and the following airplane characteristics:

Wing area, square feet	260
Span, feet	38
Taper ratio	1.67:1
Airfoil section	NACA 230 series
Mean aerodynamic chord, inches	84.14
Weight, pounds	7063
Wing loading, pounds per square foot	27.2
Stick length, feet	2
Maximum stick deflection, degrees	±21
Maximum aileron deflection, degrees:	
0.333c _a balance	±14
0.415c _a balance	±12

The value of the constant in equation (2) is dependent upon the wing loading, the size of the ailerons, and the travel of the ailerons relative to the stick. The values of C_{l_p}' and ΔC_h used in equations (1) and (2) are the values thought to exist during steady rolling; the difference in angle of attack of the two ailerons due to rolling has been taken into account.

It will be noticed in figure 10 that the variations of stick force and deflection are very nearly linear with rate of roll and that the maximum $pb/2V$ available with flaps either retracted or fully extended is greater than the minimum of 0.07 required. (See reference 4.) The high-speed stick forces appear excessive, however, and the aileron

effectiveness drops off considerably with the outboard flap in intermediate positions. Since the flap need be in the intermediate positions for only the short period during its extension or retraction, it is thought that a relatively low effectiveness for these conditions will be acceptable.

If the maximum aileron deflection is reduced to $\pm 12^\circ$ and the internal balance is increased to 0.4158, a large reduction of stick force may be obtained with only a small loss of aileron effectiveness. It was estimated from the data of figure 9 that the maximum stick force would be reduced by more than 50 percent. The $pb/2V$ would be reduced by only about 15 percent. (See fig. 11.)

Results of recent flight tests on a light airplane with an outboard flap and aileron arrangement somewhat similar to that of the present investigation (reference 5) were in general agreement with the results presented herein.

CONCLUSIONS

1. Under the conditions of the present tests the 0.58-span slotted flap provided an increment of 0.82 in maximum lift coefficient, and the 0.40-span retractable flaps over the aileron portion of the wing provided an additional increment of maximum lift coefficient of 0.22; that is, a total increment of 1.04 was given by the duplex-flap combination.
2. Deflecting the flap over the aileron portion of the wing reduced the effectiveness of the aileron at intermediate positions of the flap but not necessarily at the final position.
3. Estimated rates of roll and stick forces indicated that the wing arrangement tested would provide satisfactory lateral control on the assumed fighter airplane.

Langley Memorial Aeronautical Laboratory,
National Advisory Committee for Aeronautics,
Langley Field, Va.

REFERENCES

1. Harris, Thomas A., and Purser, Paul E.: Wind-Tunnel Investigation of Plain Ailerons for a Wing with a Full-Span Flap Consisting of an Inboard Fowler and an Outboard Retractable Split Flap. NACA A.C.R., March 1941.
2. Wenzinger, Carl J., and Harris, Thomas A.: Wind-Tunnel Investigation of an N.A.C.A. 23012 Airfoil with Various Arrangements of Slotted Flaps. Rep. No. 664, NACA, 1939.
3. Harris, Thomas A., and Purser, Paul E.: Wind-Tunnel Investigation of an NACA 23012 Airfoil with Two Sizes of Balanced Split Flap. NACA A.C.R., Nov. 1940.
4. Gilruth, R. R., and Turner, W. N.: Lateral Control Required for Satisfactory Flying Qualities Based on Flight Tests of Numerous Airplanes. Rep. No. 715, NACA, 1941.
5. Williams, W. C.: A Flight Investigation of Internally Balanced Sealed Ailerons in the Presence of a Balanced Split Flap. NACA A.R.R., May 1942.

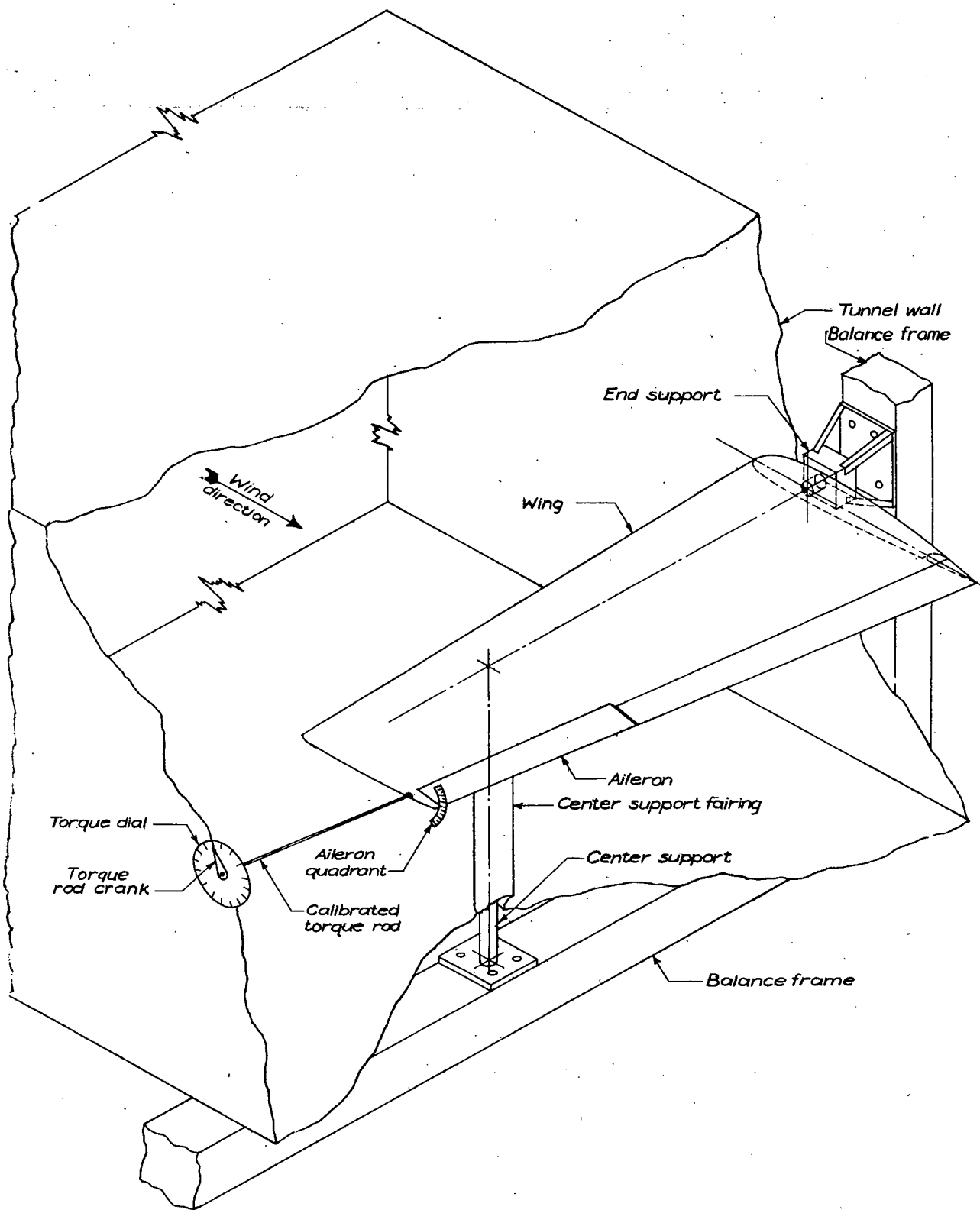
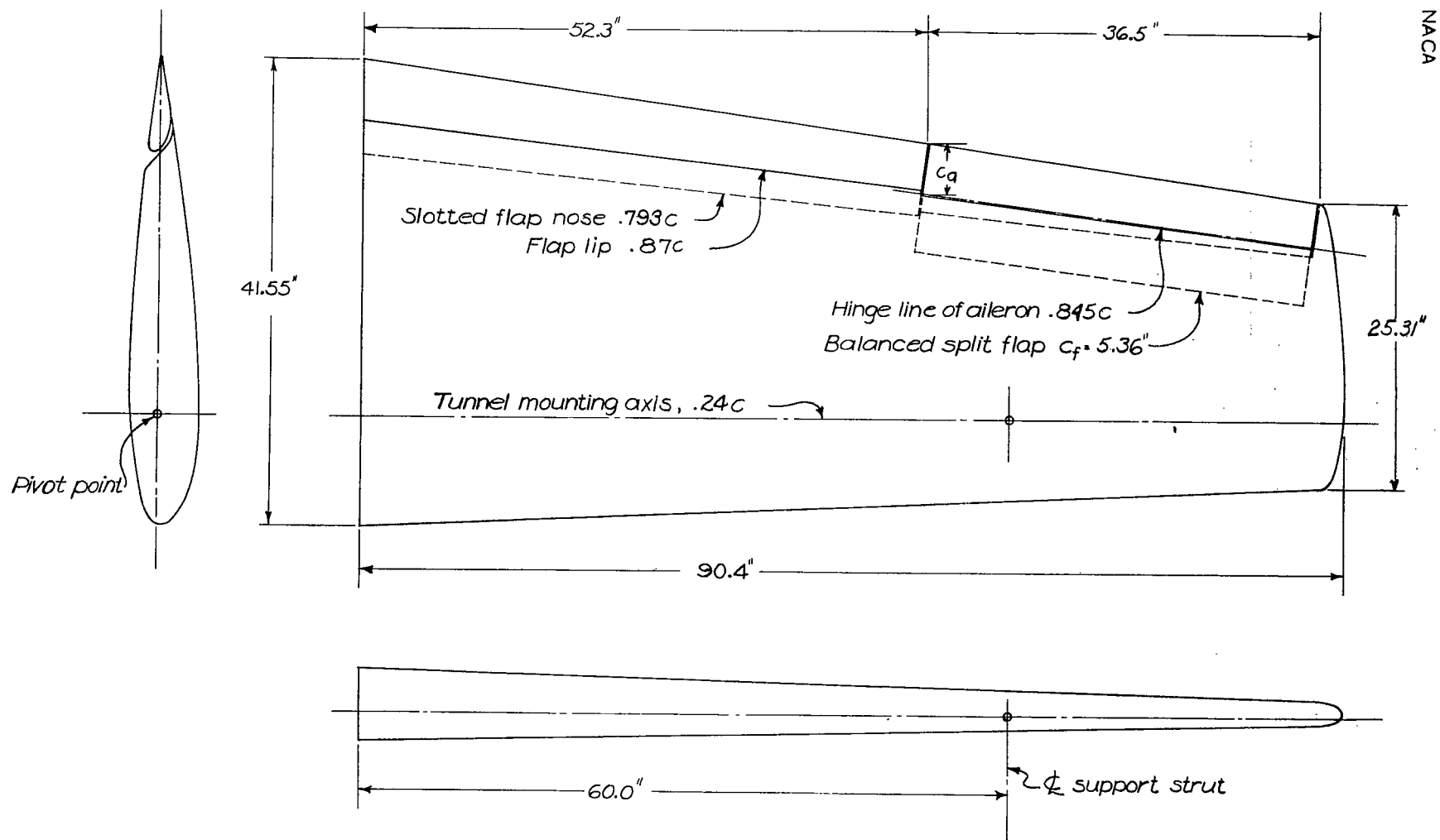
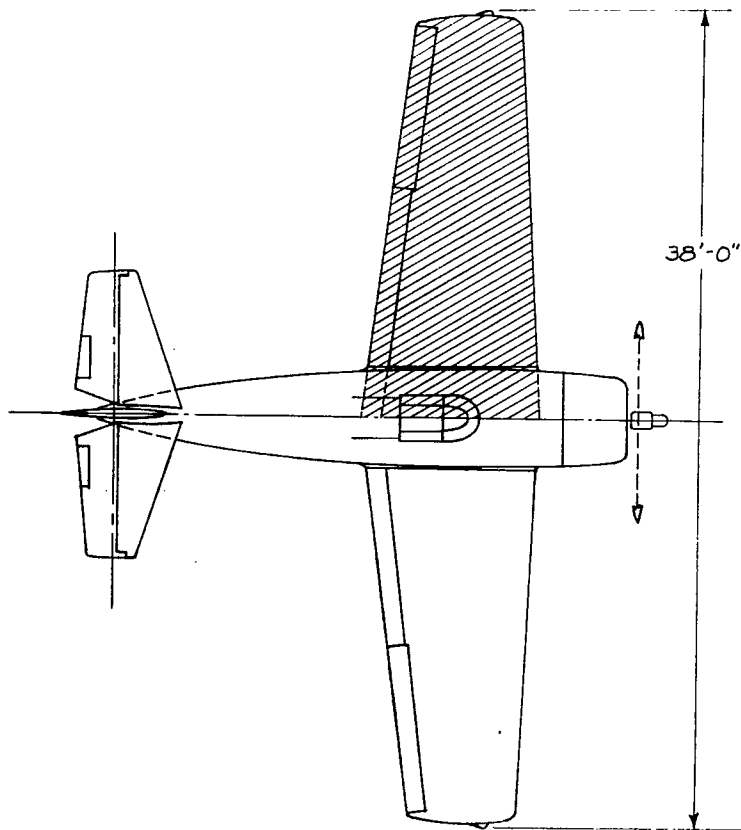


Figure 1.- Schematic diagram of test installation.



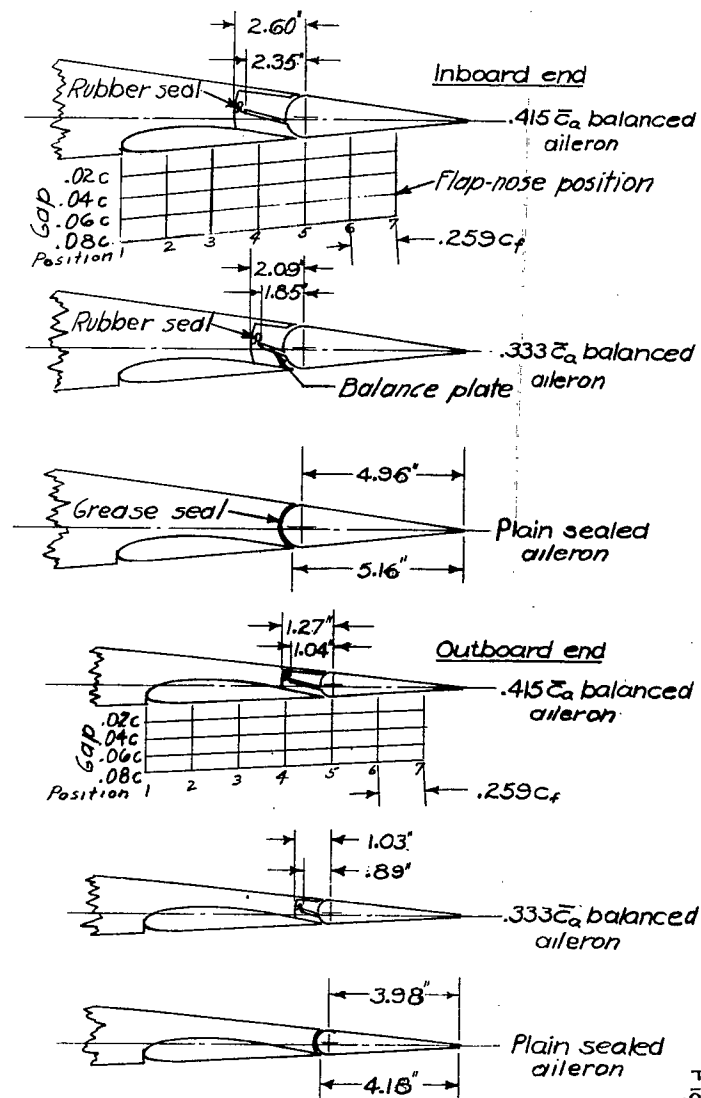
(a) General layout of model.

FIGURE 2.- Tapered wing with duplex flaps.



(b) Portion of airplane simulated by model.

FIGURE 2.- Continued.



(c) Aileron details of model.

FIGURE 2.- Concluded.

L-481

NACA

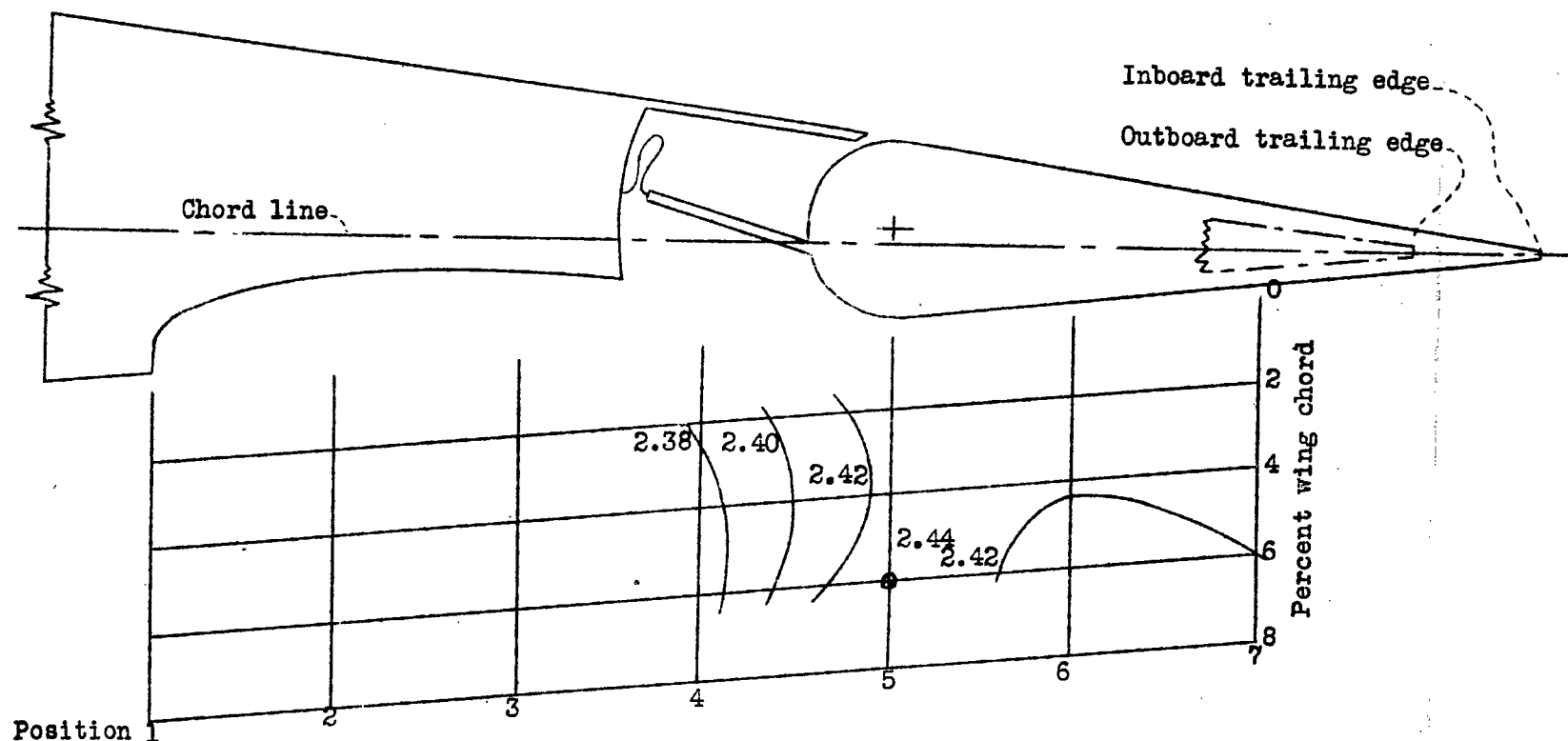
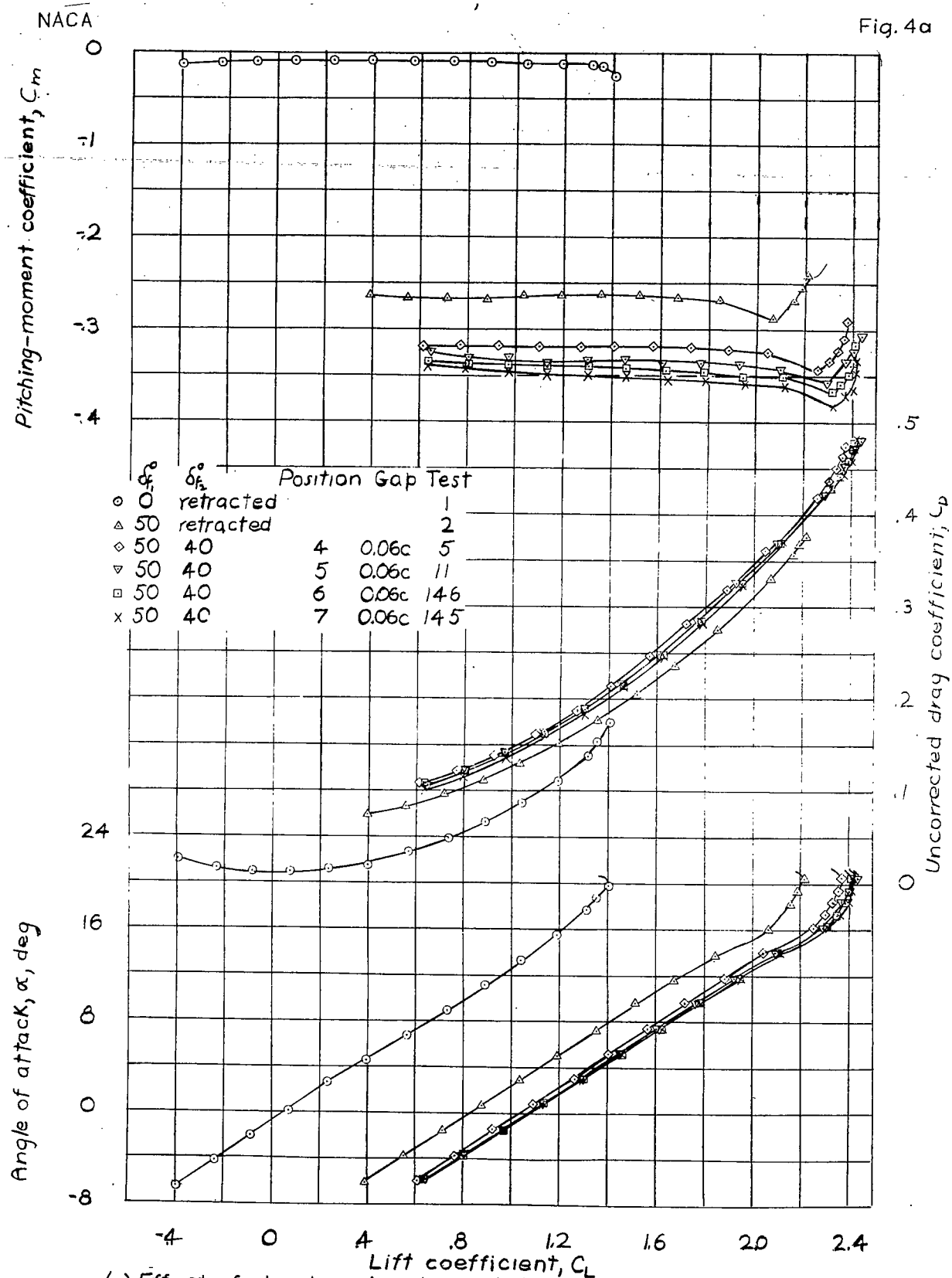
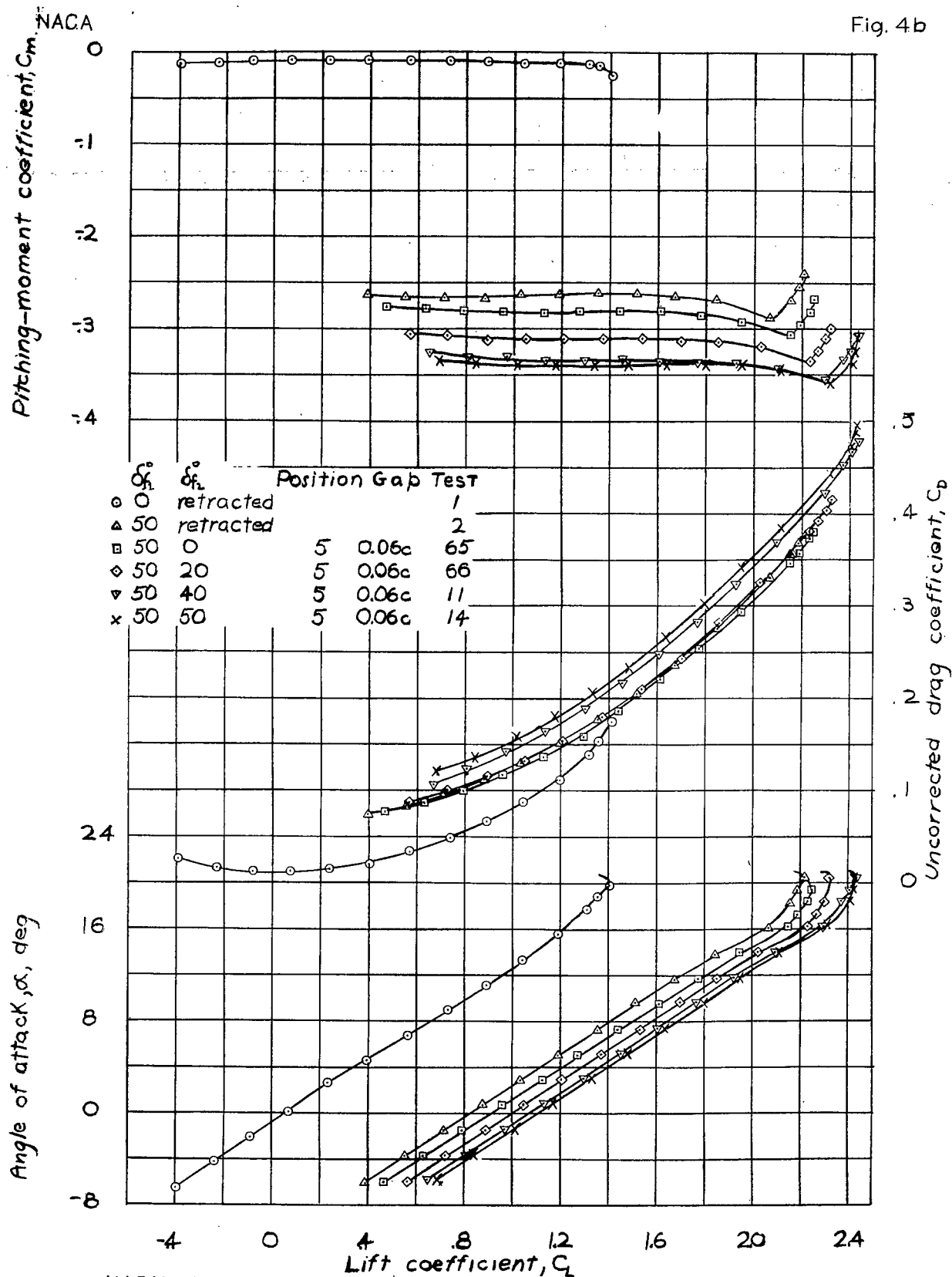


Figure 3.- Contours of outboard-flap location for maximum lift coefficient. Tapered-wing model with duplex flaps. $\delta_{f1} = 50^\circ$, $\delta_{f2} = 40^\circ$.

Fig. 3



(a) Effect of chordwise location of the outboard flap.
 Figure 4. — Lift, drag, and pitching-moment coefficients of the tapered-
 (a,b) wing model with duplex flaps.



(b) Effect of angular setting of the outboard flap.
 Figure 4. — Lift, drag, and pitching-moment coefficients of the tapered wing model with duplex flaps.

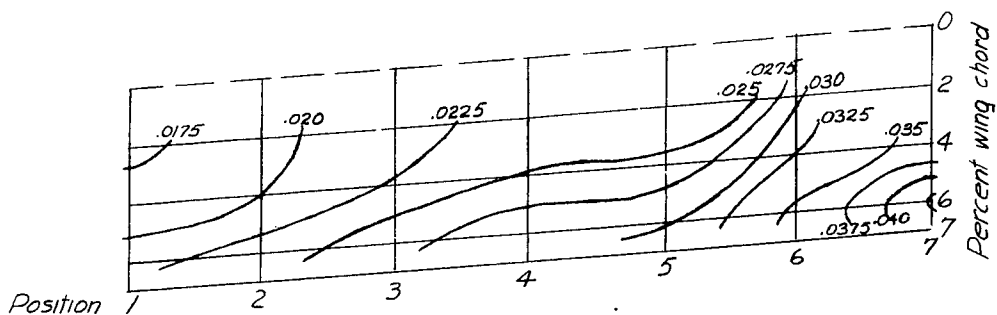
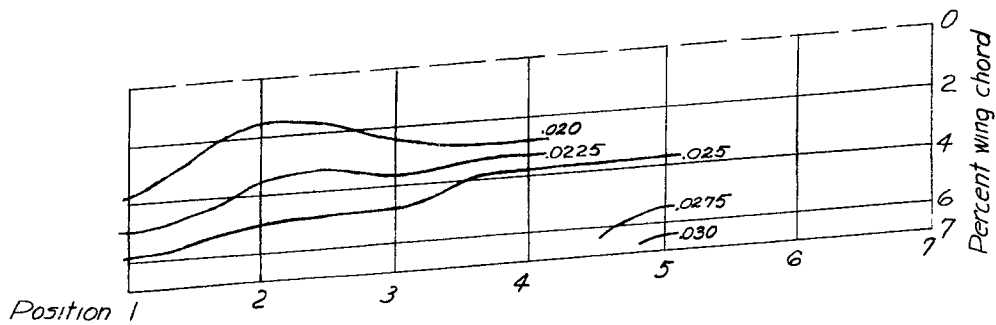
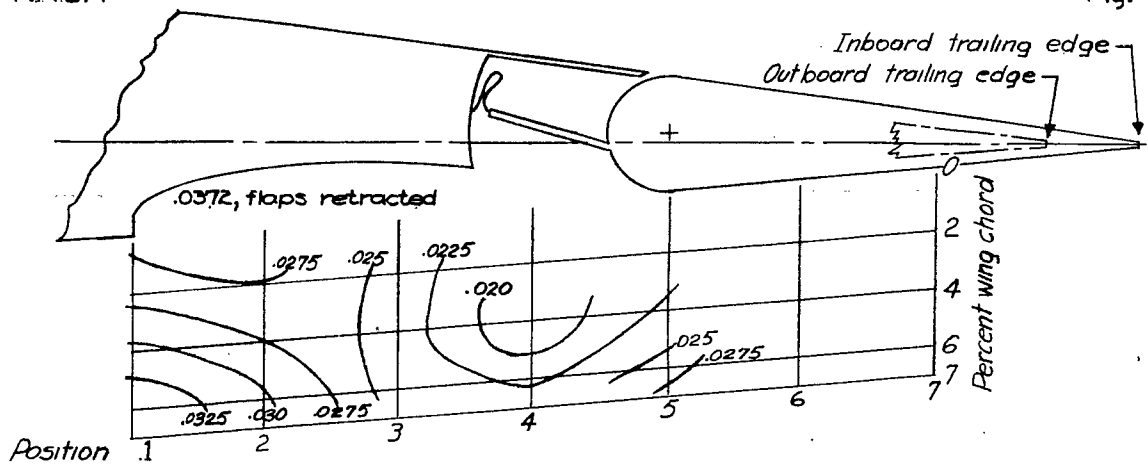
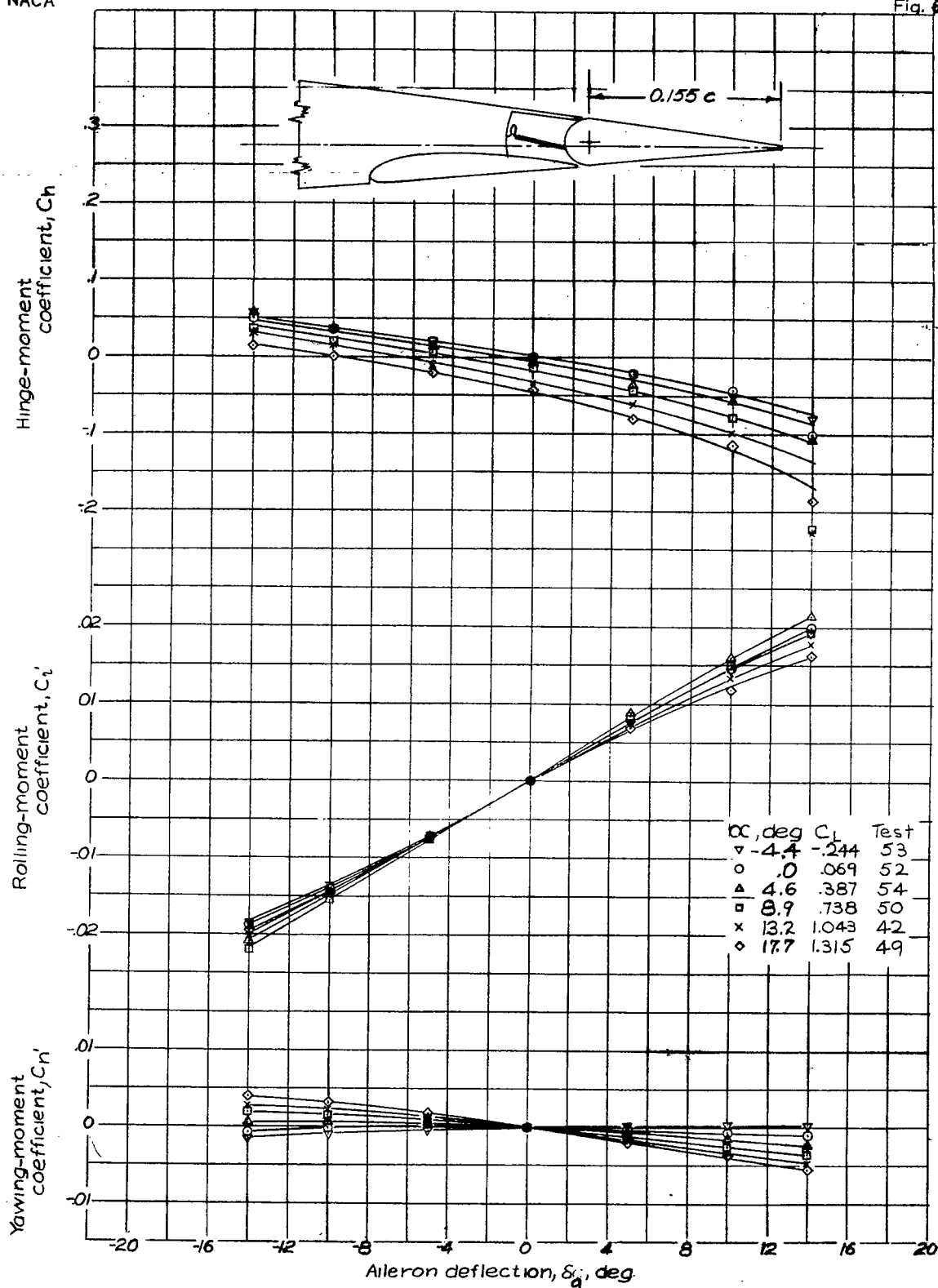
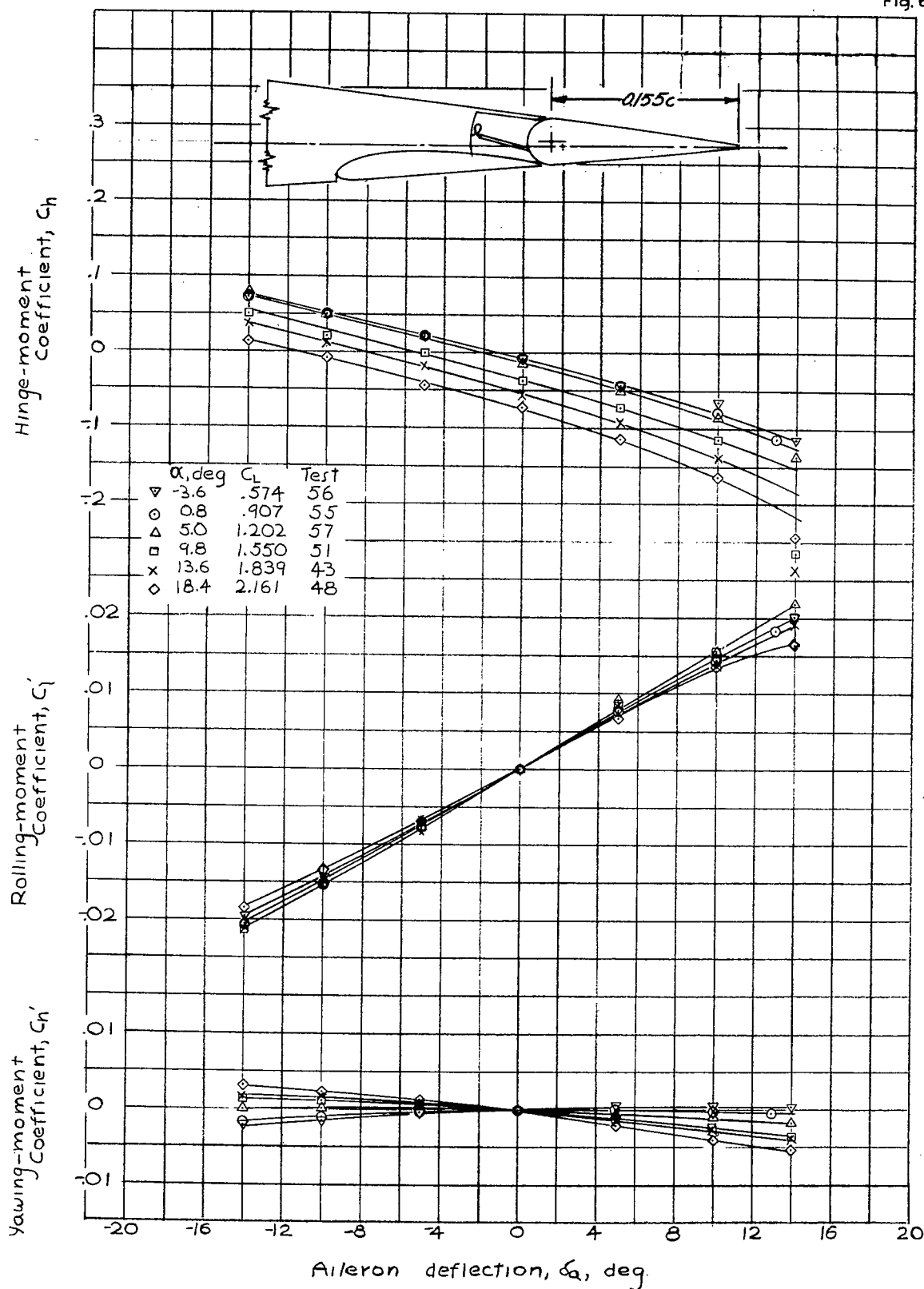


FIGURE 5.- Contours of outboard flap location for rolling-moment coefficient due to aileron deflections of $\pm 14^\circ$. Tapered-wing model with duplex flaps. $\delta_{f_1} = 50^\circ$; $\alpha = 14^\circ$.



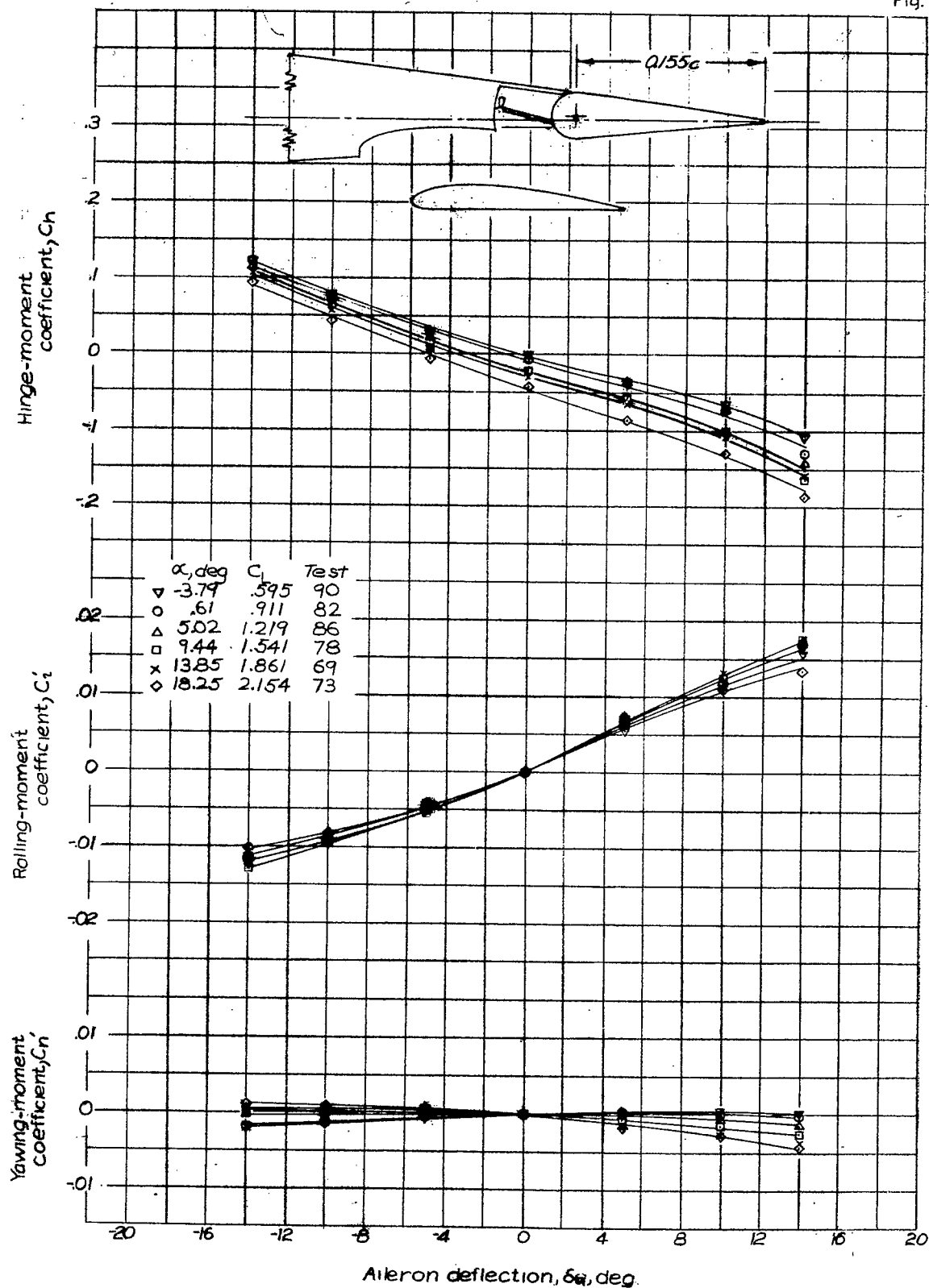
(a) Flaps retracted.

(a-h) Figure 6.- Rolling-, yawing-, and hinge-moment coefficients of the tapered-wing model with duplex flaps and $0.333\epsilon_a$ balance aileron.



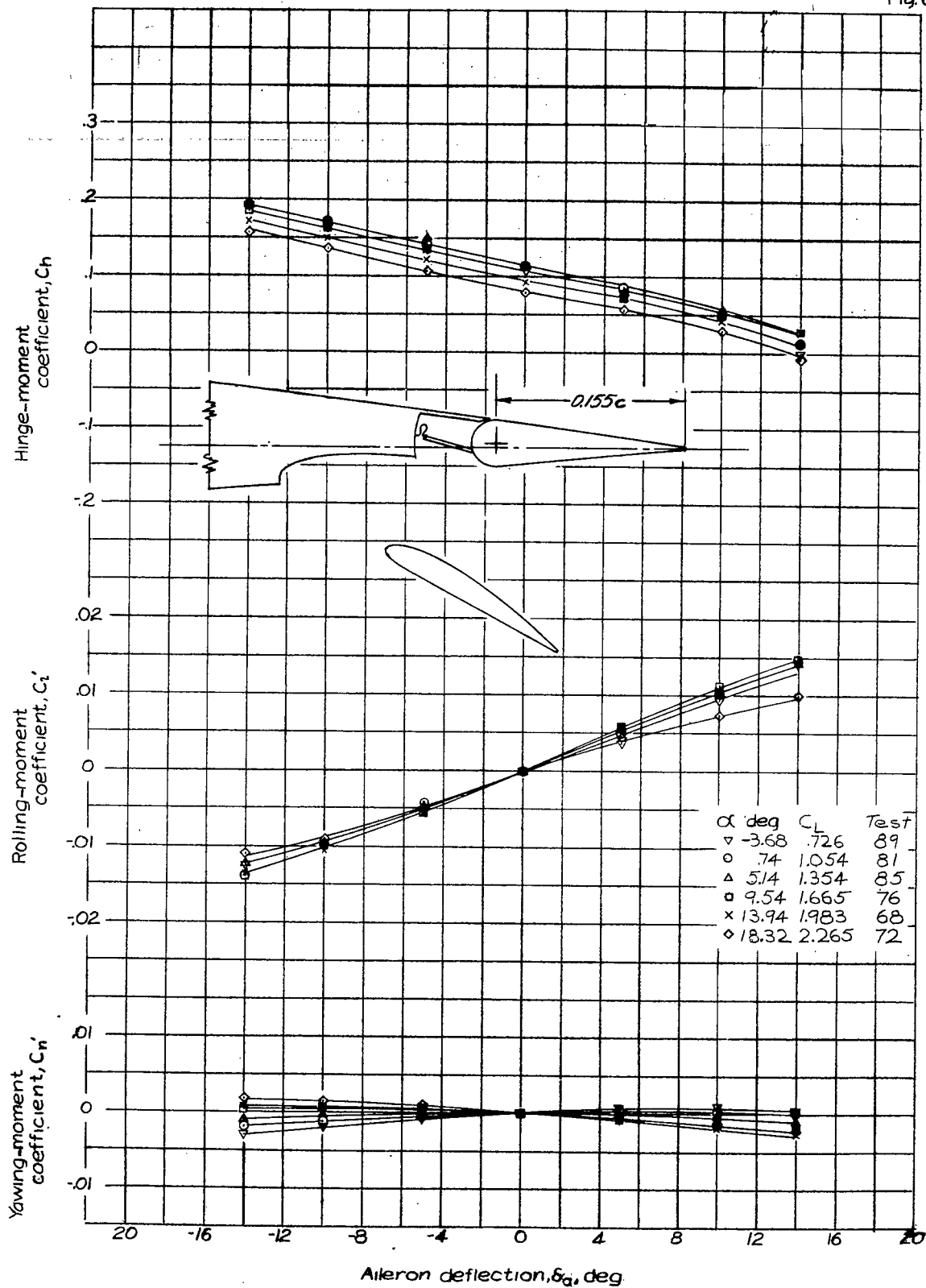
(b) Inboard flap, δ_{f1} , 50° ; outboard flap, δ_{f2} , retracted.

Figure 6.- Continued.



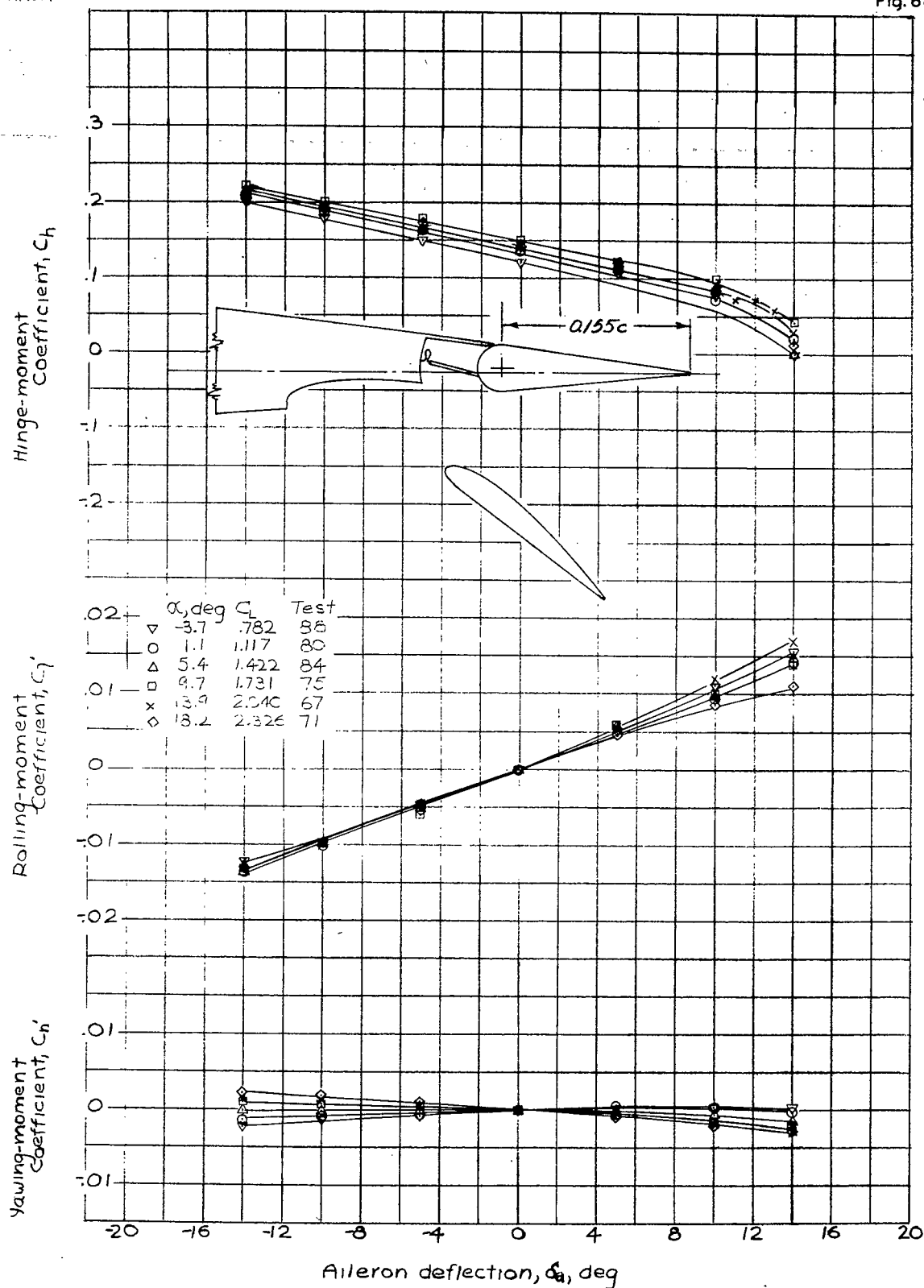
(c) Inboard flap, δ_f , 50° ; outboard flap, δ_o , 0° at position 2 with 0.04c gap.

Figure 6.- Continued.



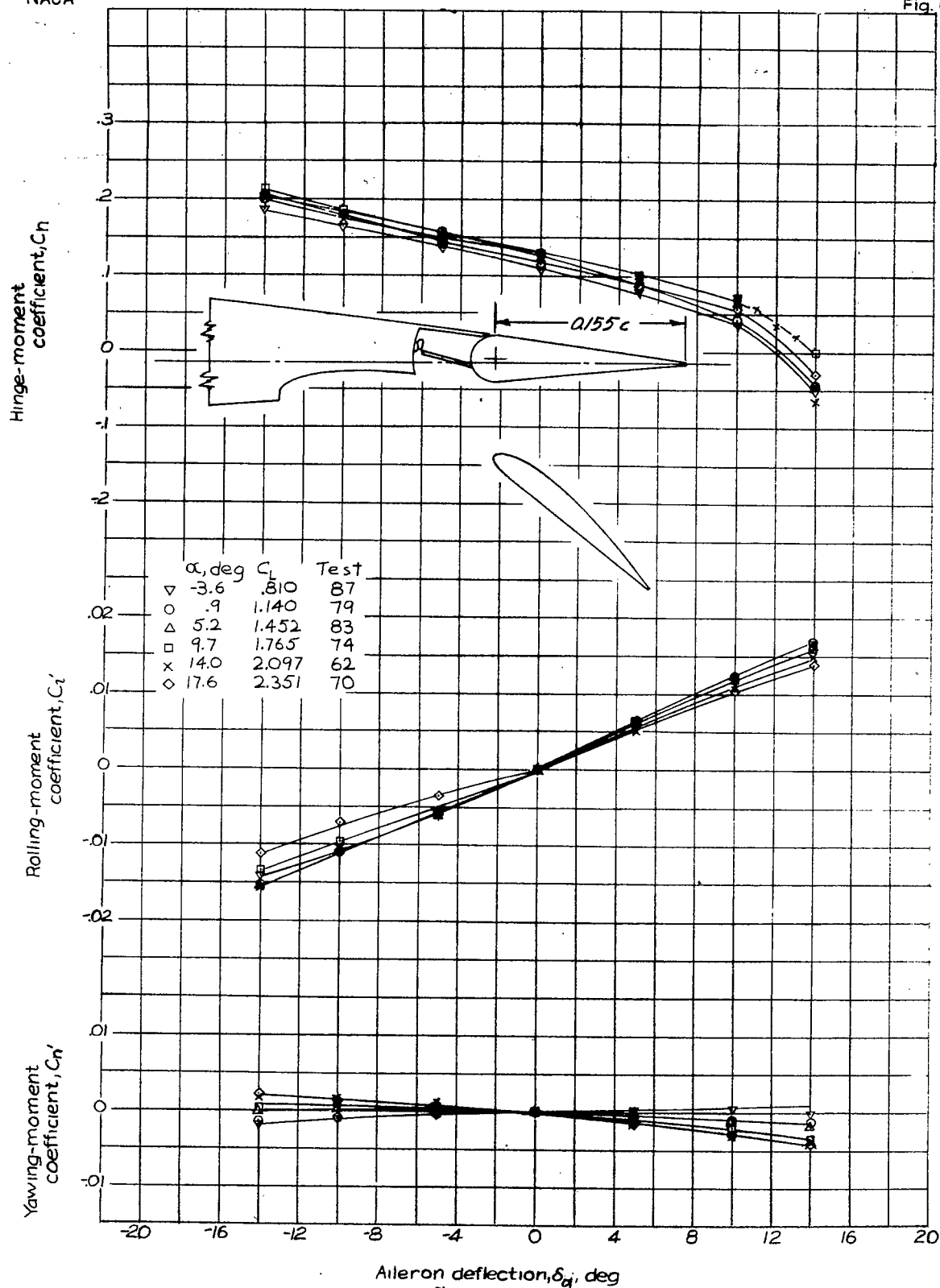
(d) Inboard flap, δ_f , 50° ; outboard flap, δ_f , 30° at position 3 with $0.06c$ gap.

Figure 6.- Continued



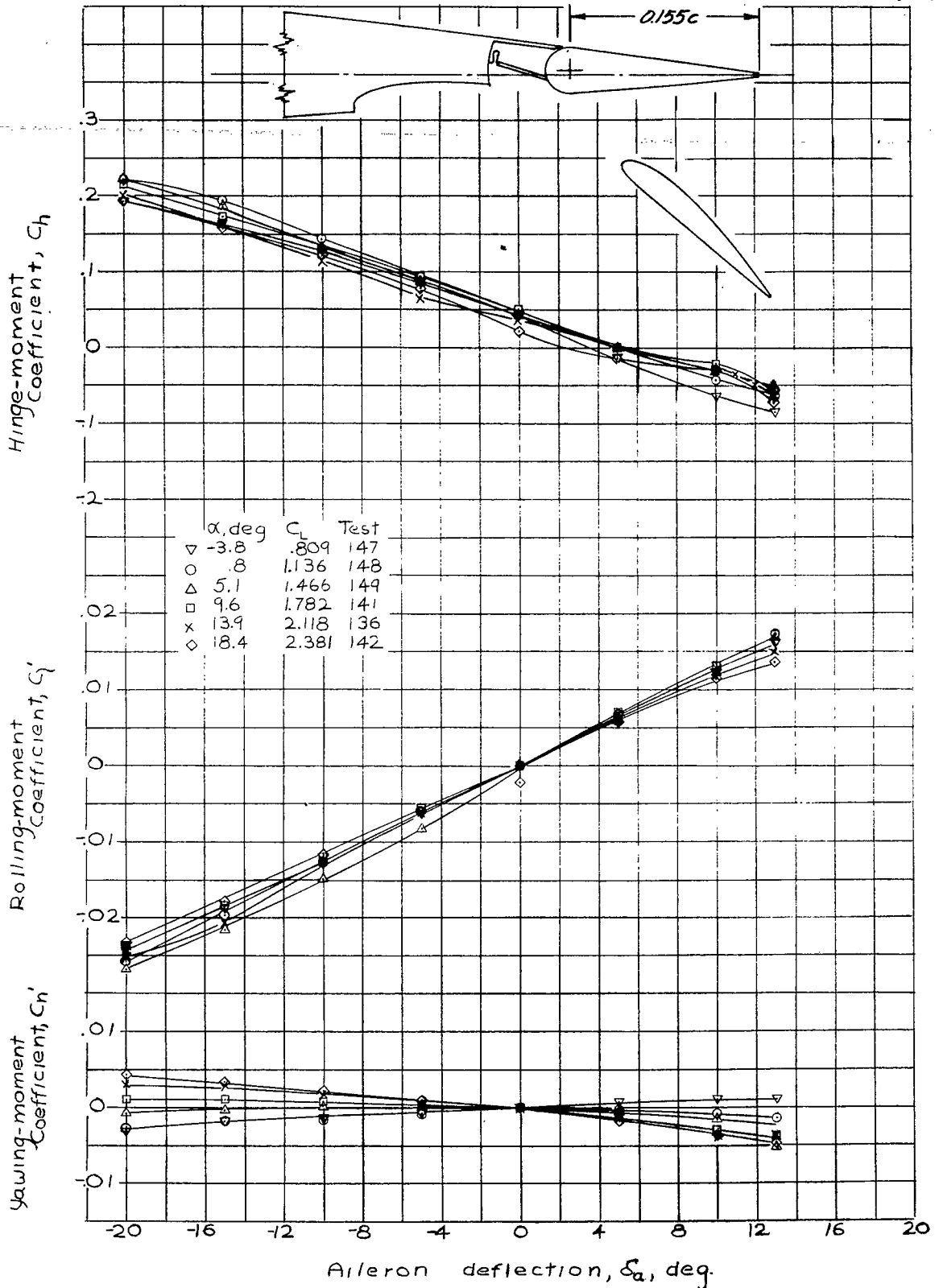
(e) Inboard flap, δ_{fi} , 50° ; outboard flap, δ_{fo} , 40° at position 4 with 0.06c gap.

Figure 6.— Continued.



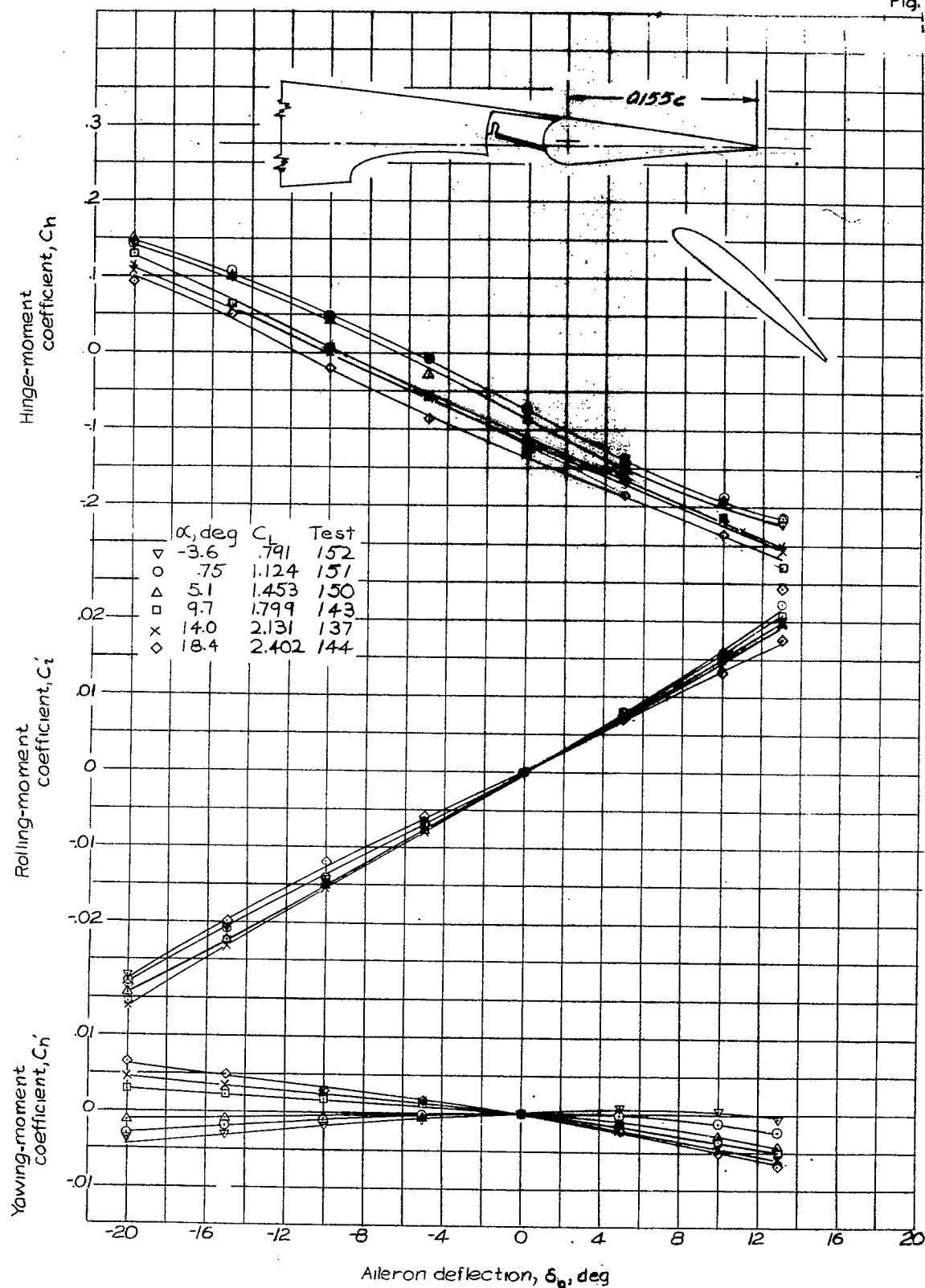
(f) Inboard flap, δ_f , 50° ; outboard flap, δ_o , 40° at position 5 with 0.06c gap.

Figure 6.- Continued.



(g) Inboard flap, $\delta_f, 50^\circ$; outboard flap, $\delta_{fe}, 40^\circ$ at position 6 with 0.06c gap.

Figure 6.- Continued.



(h) Inboard flap, δ_{fi} , 50° ; Outboard flap, δ_{fo} , 40° at position 7 with $0.06c$ gap.

Figure 6.- Concluded

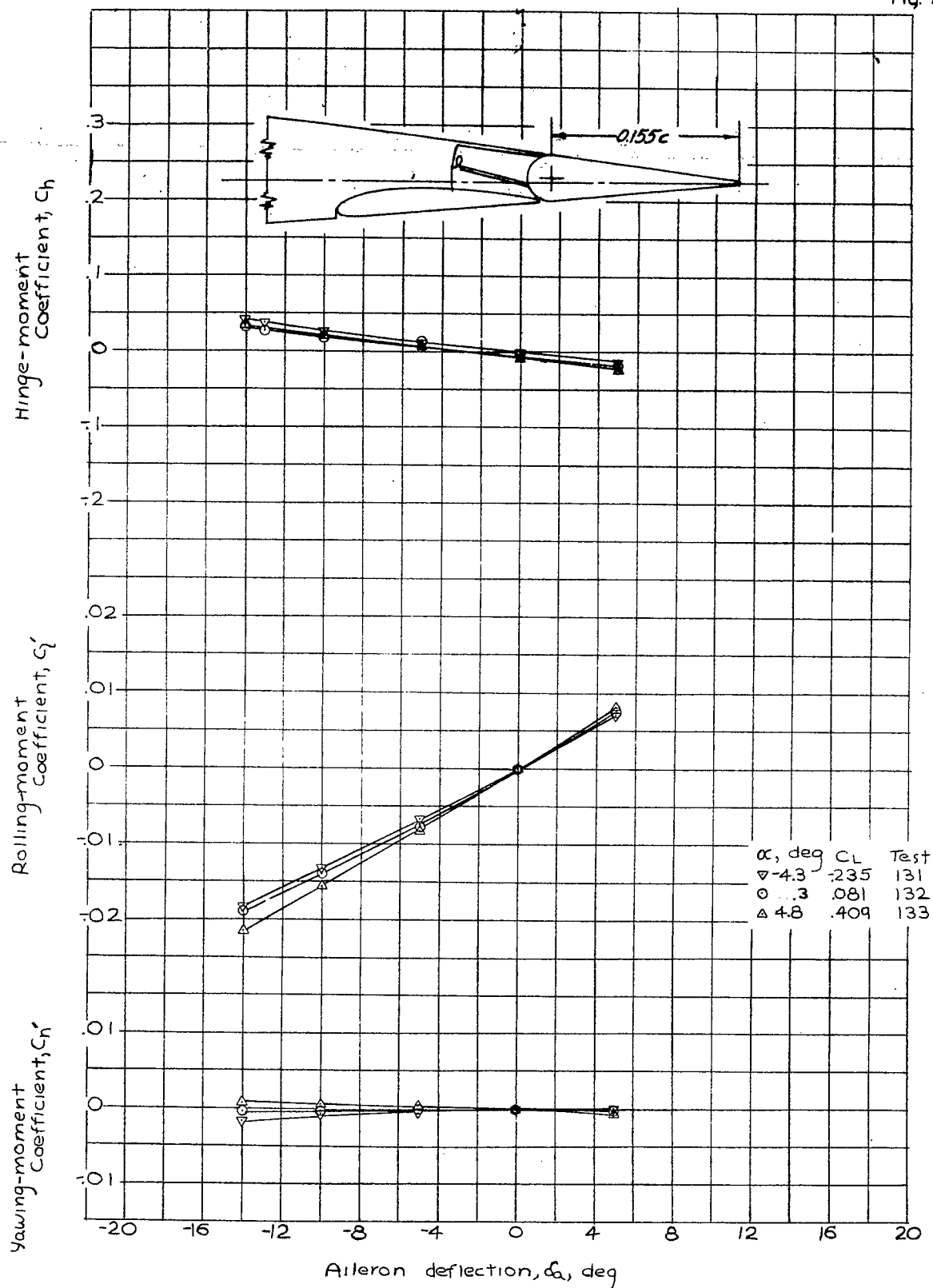
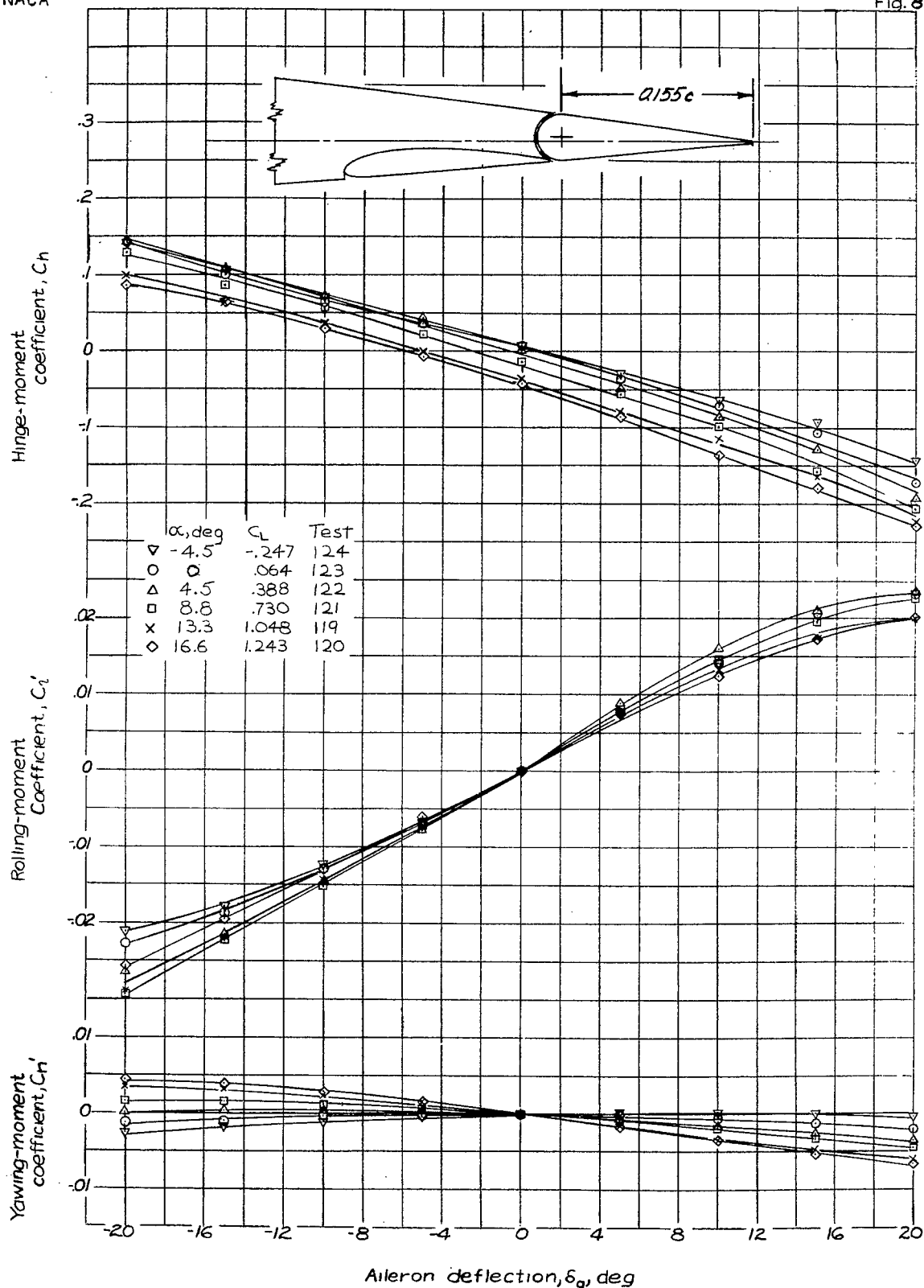
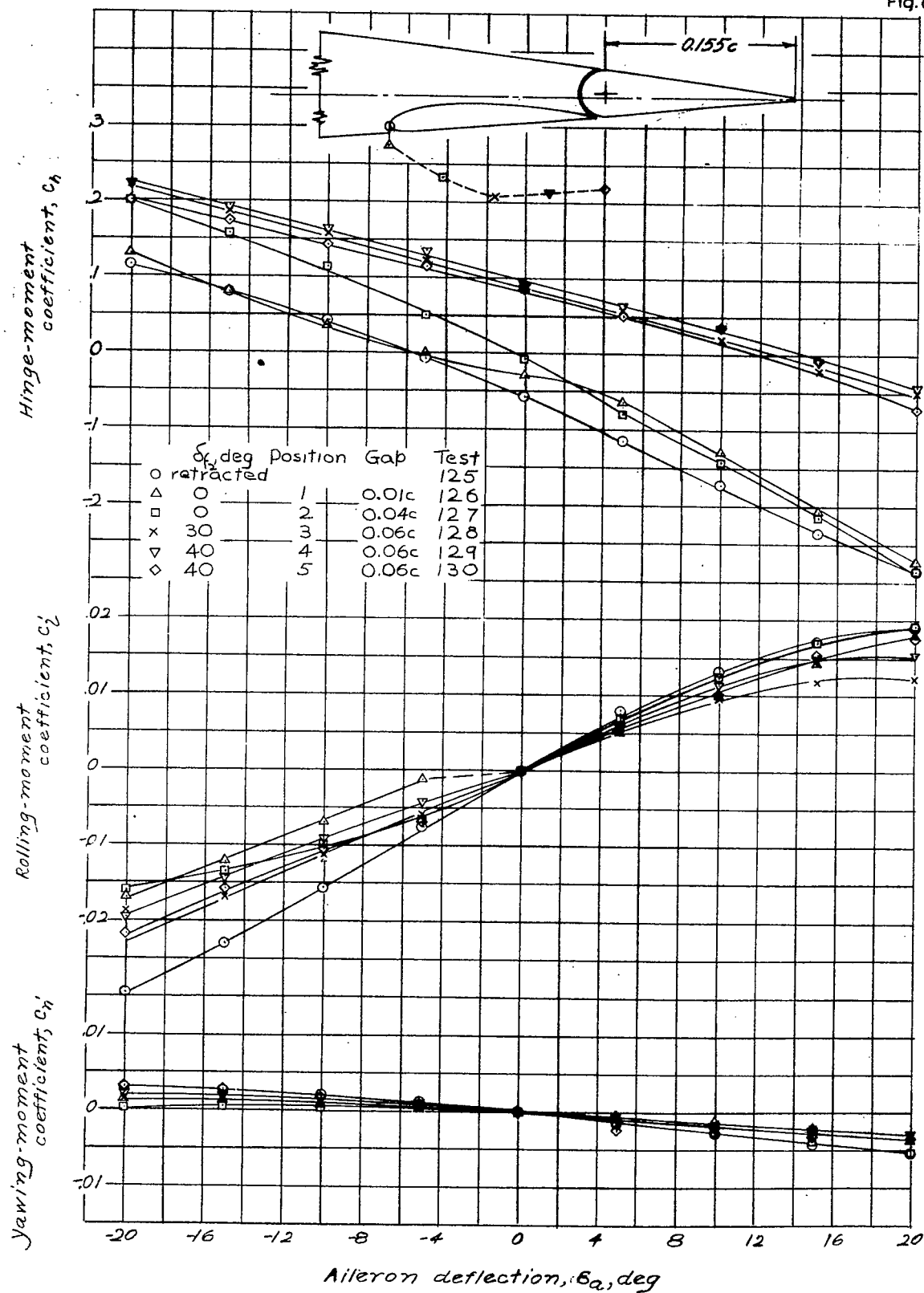


Figure 7.- Rolling-, yawing-, and hinge-moment coefficients of the tapered-wing model with duplex flaps and $0.415c_a$ balance aileron; flaps retracted.



(a) Flaps retracted.

Figure 8.- Rolling-, yawing-, and hinge-moment coefficients of the (a,b) tapered-wing model with duplex flaps and plain sealed aileron.



(b) Inboard flap, δ_f , 50° ; angle of attack, α , 13.9° .

Figure 8- Concluded,

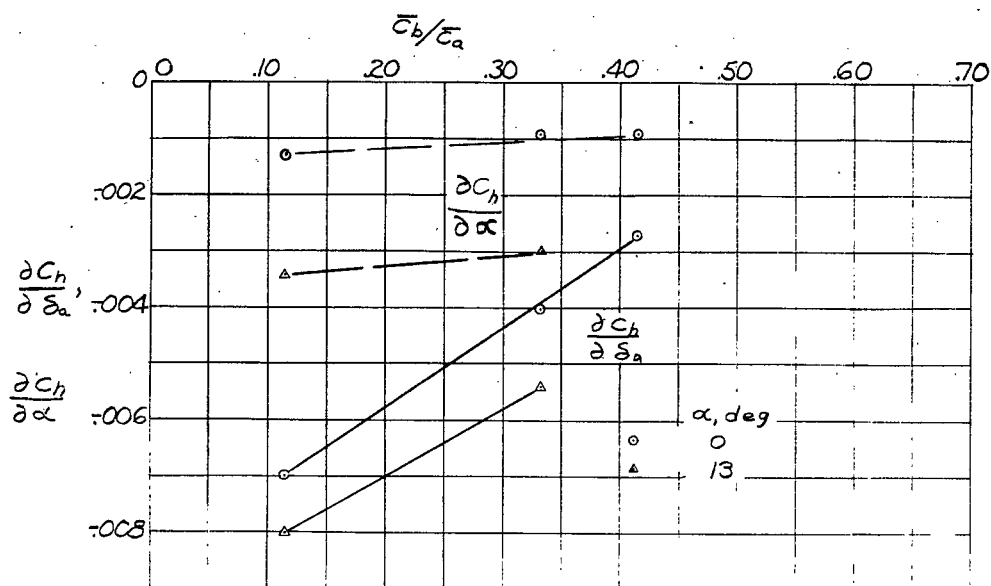


Figure 9.- Variation of $\partial C_h/\partial \alpha$ and $\partial C_h/\partial \delta_a$ with aileron balance; tapered-wing model with duplex flaps retracted.

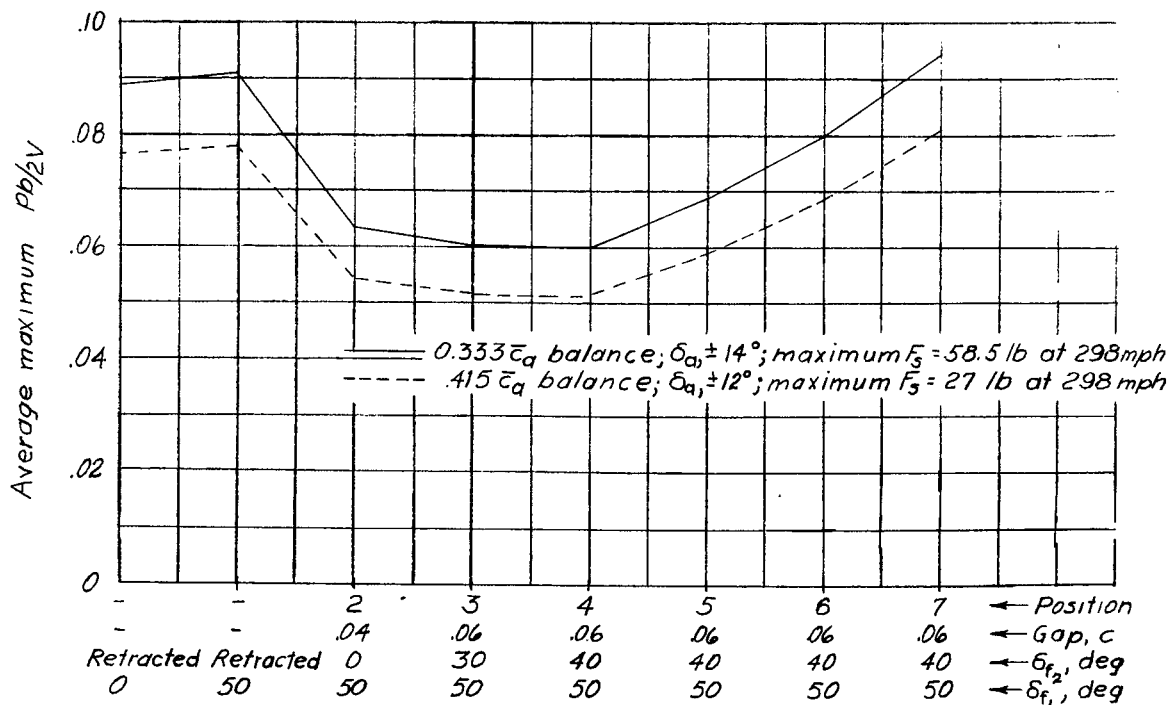


Figure 11. - Variation of estimated maximum stick force and rate of roll with maximum aileron deflection; airplane with tapered wing, duplex flaps and balanced ailerons.

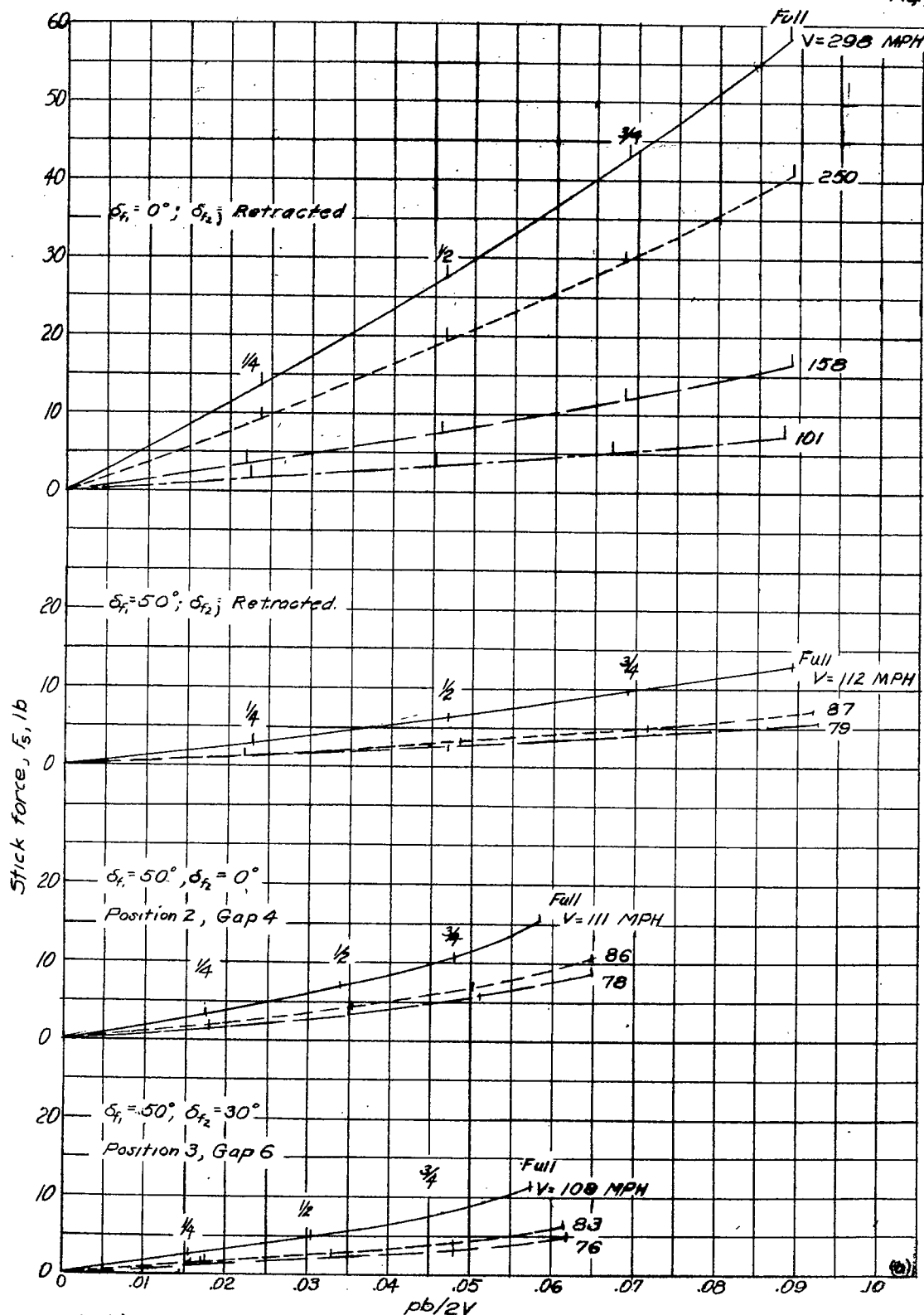


Figure 10.- Estimated aileron-control characteristics of airplane with tapered wing, duplex flaps, and $0.33Ca$ balance ailerons linked for deflection range of $\pm 14^\circ$.

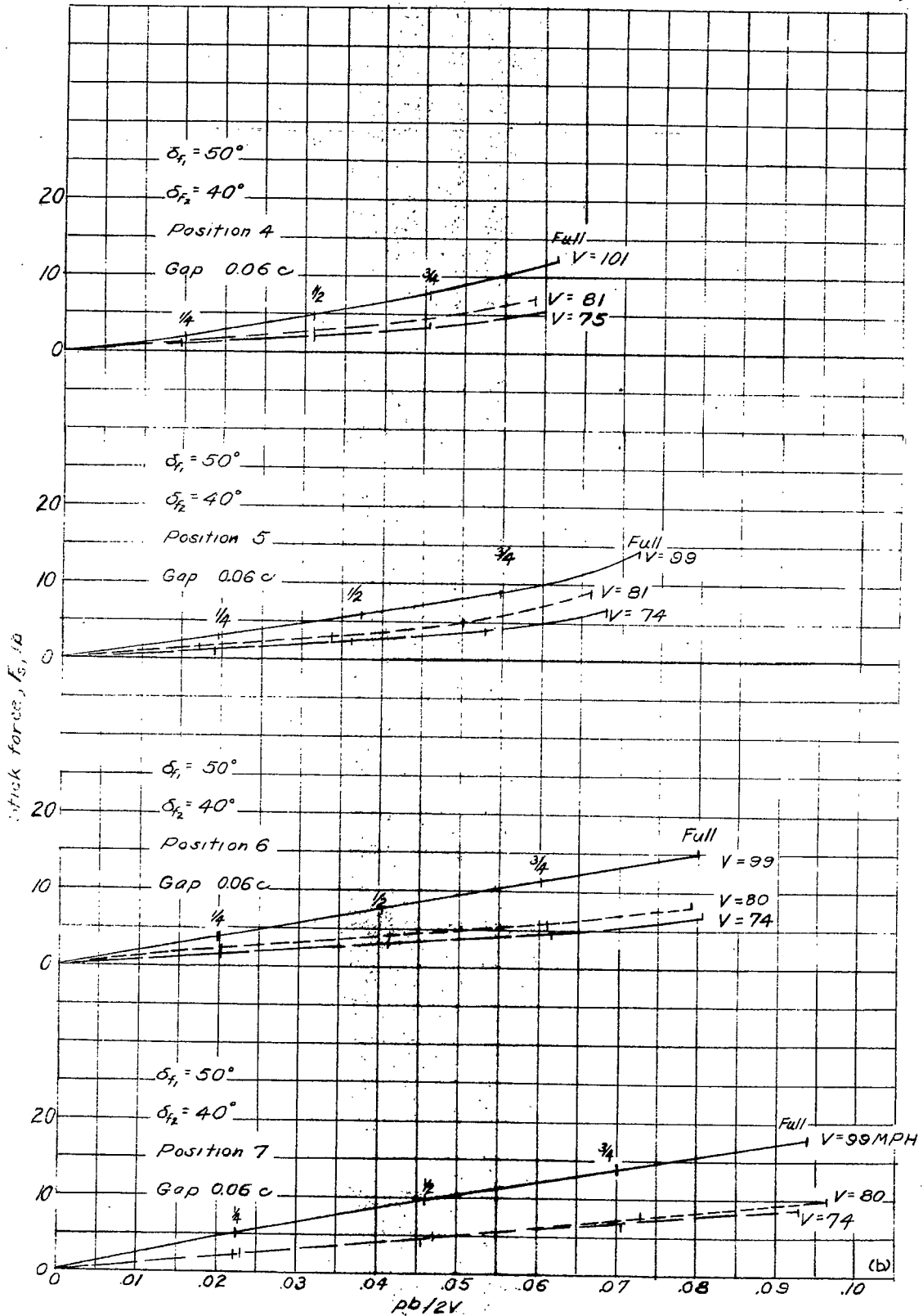


Figure 10.- Concluded

LANGLEY RESEARCH CENTER



3 1176 01354 3336